
**Separation Science and Technology**
Publication details, including instructions for authors and subscription information:
http://www.informaworld.com/smpp/title~content=t713708471

# Thermal Swing Adsorption Process to Minimize the Thermal Pulse During the Feed Step

R. Kumar[a]; V. Koss[a]; N. Perelman[a]; I. Ioffe[a]
[a] THE BOC GROUP, GASES TECHNOLOGY, NEW JERSEY, USA

Online publication date: 11 September 2000

**To cite this Article** Kumar, R. , Koss, V. , Perelman, N. and Ioffe, I.(2000) 'Thermal Swing Adsorption Process to Minimize the Thermal Pulse During the Feed Step', Separation Science and Technology, 35: 14, 2279 — 2297
**To link to this Article: DOI:** 10.1081/SS-100102102
**URL:** http://dx.doi.org/10.1081/SS-100102102

SEPARATION SCIENCE AND TECHNOLOGY, **35**(14), pp. 2279–2297, 2000

# Thermal Swing Adsorption Process to Minimize the Thermal Pulse During the Feed Step

R. KUMAR,* V. KOSS, N. PERELMAN, and I. IOFFE
THE BOC GROUP
GASES TECHNOLOGY
100 MOUNTAIN AVE., MURRAY HILL, NEW JERSEY 07974, USA



## ABSTRACT

At the start of the feed step, thermal swing adsorption (TSA) processes generate a thermal pulse. This thermal pulse is generated by insufficient cooling of the bed during the regeneration step and bed repressurization following the cooling step. For some integrated processes, such as cryogenic air separation units (ASU), the thermal pulse generated by the TSA PPU (pre-purification unit) may not be acceptable. Three options are outlined to minimize the magnitude of the thermal pulse generated by the adsorbent bed during the feed step before the feed enters the equipment downstream of the adsorption process. A mathematical model to simulate this process and results from computer simulations are presented. Various process options are compared. Experimental data is compared against the model predictions.

## INTRODUCTION

Thermal swing adsorption (TSA) processes are used to remove trace impurities from a bulk gas stream. One example of such an application is the removal of water, carbon dioxide, and other trace impurities from air before its fractionation by cryogenic distillation to produce nitrogen, oxygen, argon, and other industrial gases. The TSA process for air purification, carried out in multiple beds, usually has the following five steps:

1. **Feed** step: compressed air is fed through the bed packed with adsorbents capable of removing the trace contaminants from air. Clean air from the adsorbent bed is then fed to other units of the air-separation plant, such as

* To whom correspondence should be addressed.

the heat exchanger, secondary air compressor, etc., before being sent to the cryogenic distillation column.

2. **Depressurization** step: the pressure of the adsorbent bed saturated with air contaminants is reduced from the feed pressure to a lower pressure, usually close to the ambient level.
3. **Heating** step: the temperature of the adsorbent bed is raised to levels such that the adsorbed air contaminants are desorbed from the adsorbent bed. This step is carried out by flowing a hot clean gas in a direction opposite to the feed flow.
4. **Cooling** step: the temperature of the adsorbent bed is reduced to feed temperature to get the adsorbent bed ready for the next feed step. This step is carried out by flowing a cold clean gas in a direction opposite to the feed flow.
5. **Repressurization** step: the pressure of the regenerated clean adsorbent bed is increased from the regeneration pressure, usually ambient, to feed pressure. This bed is now ready to go to the feed step again, whereas the other bed starts on the depressurization step.



The regeneration gas used in steps 3 and 4 for the heating and the cooling steps is usually part of the contaminant-free product gas. Therefore, every attempt is made to minimize the regeneration gas quantity. Also, the power consumption is reduced with the regeneration gas quantity. However, there are two limits on the minimum amount of the regeneration gas required. The first limit is based on the total heat input as required during the third step. If enough heat is not supplied, the adsorbent is not properly regenerated for the next feed step. The second limit, generally *not* recognized in the literature, is based on the cooling required in the fourth step. If the bed is not cooled properly, a thermal pulse is generated when that bed starts on the feed step during the next cycle. Even though from adsorption point of view (1) the cooling step may not be necessary, the equipment downstream of the TSA unit may not be able to handle the thermal pulse caused by insufficient cooling.

The second source responsible for generating the thermal pulse is the repressurization step. Feed air, or the product air generated during the feed step, is used for bed repressurization during the fifth step. At least one of the adsorbents used in the TSA PPU beds in front of the ASUs is a zeolite. Therefore, the temperature of the bed rises significantly during the repressurization step due to the heat of air adsorption on the zeolite. Figure 1 plots the temperature rise due to air adsorption in a typical bed packed with NaX zeolite. Because the large-diameter adsorbent beds are adiabatic, this heat also exits the adsorbent bed as a thermal pulse when this bed is put on the next feed step.

In the following, a mathematical model is used to simulate various cycle options to minimize the magnitude of the thermal pulse exiting the adsorbent

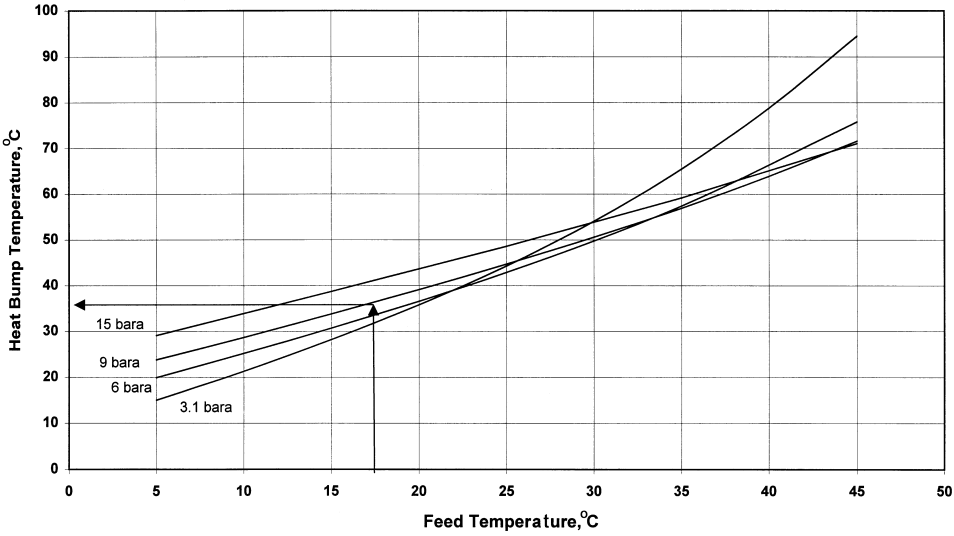


FIG. 1 Expected temperature rise due to repressurization by air. *P* initial ~1 bara; parameter = feed pressure.



bed. In all the options, the bed is completely regenerated and the regeneration gas requirement is minimized.

## MATHEMATICAL MODEL

Mathematical description of the process is based on mass and energy conservation laws (2, 3). The following assumptions are made:

1. Ideal gas law applies.
2. Thermal equilibrium is assumed between the gas, the adsorbent, and the vessel walls.
3. Pressure gradients inside the bed are neglected.
4. No variation exists in the radial direction for both concentration and temperature.
5. The linear-driving-force model is applicable to describe the rate of mass transfer.
6. Dispersion terms are small with respect to convection terms.
7. The vessel is thermally insulated from the ambient.
8. Gas velocity in the bed can be calculated as a function of temperature according to the gas flow conservation law and the ideal gas equation. The velocity changes because adsorption or desorption of the trace impurities is neglected.

The mass balance is given by (4)

$$\varepsilon_j \frac{\partial C_i}{\partial t} + \varepsilon_j \frac{\partial \mathrm{u} C_i}{\partial x} - (1 - \varepsilon_j)\, S_j^i = 0 \tag{1}$$

$$\rho_j \frac{\partial Q_j^i}{\partial t} + S_j^i = 0 \tag{2}$$

Linear driving force approximation is used for the rate of adsorption

$$S_j^i = -\rho_j K_j^i (Q_j^{i\mathrm{eq}} - Q_j^i) \tag{3}$$

where, $u$ denotes interstitial velocity, $C$ denotes concentration, $\rho$ denotes adsorbent bulk density, $\varepsilon$ denotes void fraction for the adsorbent, $Q$ denotes moles of adsorbed component, $S$ denotes adsorption rate, and indices $i$ and $j$ denote gas species and adsorbent, respectively. Index eq refers to equilibrium.

The equilibrium isotherms are given by the following expression

$$Q^{\mathrm{eq}} = \sum_{i=1}^{3} \frac{b_i m_i}{1 + b_i} \tag{4}$$

where, $b_i = B_i \exp[\Delta H_j^i/(RT)]$
where $b$, $B$, $m$, and $\Delta H_j^i$ are constants.

Thermal effects associated with the process are taken into account by using energy conservation for the bed

$$\left(\varepsilon_j C_{pg} C + (1 - \varepsilon_j) C_j^s \rho_j + (1 - \varepsilon_j) C_{pg} \rho_j \sum_{i=1}^{N} Q_j^i\right)$$
$$\frac{\partial T}{\partial t} + \varepsilon_j C_{pg} C\, u \frac{\partial T}{\partial x} + (1 - \varepsilon_j)\rho_j \sum_{i=1}^{N} \Delta H_j^i S_j^i + \frac{4 h_w}{d_{\mathrm{in}}} (T - T_w) = 0 \tag{5}$$

and the wall

$$\rho_w C_w \frac{\partial T_w}{\partial t} - \frac{16 h_w d_{\mathrm{in}}}{\pi (d_{\mathrm{out}}^2 - d_{\mathrm{in}}^2)} (T - T_w) = 0 \tag{6}$$

Here $T$ denotes temperature, $C_{pg}$ denotes gas heat capacity at constant pressure, $\Delta H$ denotes heat of adsorption, $h$ denotes heat transfer coefficient, $d_{\mathrm{in}}$ and $d_{\mathrm{out}}$ denote inner and outer bed shell diameters, respectively, and indices $w$ and $S$ refer to the wall and solid adsorbent, respectively.
Integration of Eqs. (1)–(6) starts with the initial conditions

$$\begin{gathered} C_i(x, t = 0) = C_{io}, \\ Q_j^i(x, t = 0) = 0, \\ T\,(x, t = 0) = T_o \text{ and} \\ T_w\,(x, t = 0) = T_o \end{gathered} \tag{7}$$

The computational time for the solution of this problem is prohibitive. The reason for this behavior, as analysis shows, is the multiplicity of very different characteristic times describing the adsorption. The characteristic times differ by orders of magnitude. However, the multitude of characteristic times' magnitude provides a solution for the speed-up of the numerical calculations. In the model, kinetics of nitrogen adsorption–desorption, by far the fastest, is substituted for local equilibrium.

### Repressurization and Depressurization steps

For repressurization and depressurization steps, only nitrogen is taken into account, because the thermal effect of water and $CO_2$ adsorption is small in comparison with nitrogen during these steps. The description of these steps includes calculations of pressure, temperature, and gas velocity. Conservation of mass and energy, as described by Eq. 1–6, is used along with the following equation that combines the expressions for compressible gas flow with overall mass balance in the bed

$$\varepsilon \frac{\partial P}{\partial t} \int_0^L \frac{dx}{RT} + (1z - \varepsilon)\, \rho_b \int_o^L dx \frac{\partial Q(P,T)}{\partial t} = \frac{S_{\text{orifice}}}{S_{\text{bed}}} G(P_{\text{out}},T_{\text{out}},P_{\text{to}}) \quad (8)$$

where,

$$G = \left(\frac{2}{\gamma + 1}\right)^{\frac{\gamma+1}{2(\gamma-1)}} \frac{P_{\text{from}}}{RT_{\text{from}}}\, s\,(T_{\text{from}}) \qquad \text{if } P_{\text{to}} < P_{\text{cr}}$$

$$G = \left(\frac{2}{\gamma - 1}\right)^{1/2} \left(\frac{P_{\text{to}}}{P_{\text{from}}}\right)^{1/\gamma} \frac{P_{\text{from}}}{RT_{\text{from}}} \left[1 - \left(\frac{P_{\text{to}}}{P_{\text{from}}}\right)^{\frac{\gamma-1}{\gamma}}\right]^{1/2} s(T_{\text{from}}) \qquad \text{if } P_{\text{to}} \geq P_{\text{cr}}$$

$$P_{\text{cr}} = \left(\frac{2}{\gamma + 1}\right)^{\frac{\gamma}{(\gamma-1)}} P_{\text{from}}$$

Here indices to and from refer to parameters with respect to flow direction, $s(T)$ denotes sonic velocity at temperature $T$, $S_{\text{bed}}$ denotes bed cross-section, $S_{\text{orifice}}$ denotes orifice cross-section, and $\gamma$ is ratio of gas heat capacities at constant pressure and volume.

## NUMERICAL PROCEDURE

For adsorption–desorption steps the system of partial differential equations (1–6) was solved numerically using four-point biased upwind differencing routine DSS018 from the DSS/2 package (5), and LSODES integrating routine (6). Equations for the repressurization and depressurization steps, after

discretization, were integrated using the forward Euler scheme. Equation 8 was discretized as follows:

$$\varepsilon \frac{P_i^{k+1} - P_i^k}{\Delta t} \sum_{i=0}^{N} \frac{\Delta x}{RT_i^k} + (1 - \varepsilon)\rho_b \sum_{i=0}^{N} \Delta x \frac{Q(P_i^k, T_i^k) - Q(P_i^{k-1}, T_i^{k-1})}{\Delta t} = \frac{S_{\text{orifice}}}{S_{\text{bed}}} G(P_{\text{from}}^{k+1}, T_{\text{from}}^k, P_{\text{to}}^{k+1}) \tag{9}$$

Here lower index $i$ denotes spatial discretization, and upper index $k$ denotes time step.

## RESULTS AND DISCUSSIONS

### Model Validation

The simulator described above was used for simulating a TSA PPU in front of an air-separation plant. Table 1 lists the operating conditions used for data collection in the plant. For this experiment, the adsorbent bed was not cooled sufficiently during the regeneration step. Following the regeneration and the repressurization steps, the temperature profiles inside the bed were measured at four locations as a function of time. The measured data points are plotted in Fig. 2. The results from the simulator are also plotted for comparison (solid lines). This is a true prediction and not a fit. It is observed from Fig. 2 that the simulator reasonably predicts the magnitude and transient behavior of temperature peaks at different locations inside the TSA PPU adsorbent bed during the feed step. The experimental data also shows that the magnitude of the thermal peak could be quite high if the bed is not properly cooled.

TABLE 1
Operating Conditions for the Plant Test

| | | |
|---|---|---|
| Feed pressure | 10.4 | bara |
| Feed temperature | 21 | °C |
| Feed flow rate | 2769 | SCMH |
| Regeneration temperature | 204 | °C |
| Regeneration flow rate | 180 | SCMH |
| Total adsorbent weight | 2426 | kg/bed |
| Vessel ID | 1.12 | m |
| Vessel T-T | 4.1 | m |

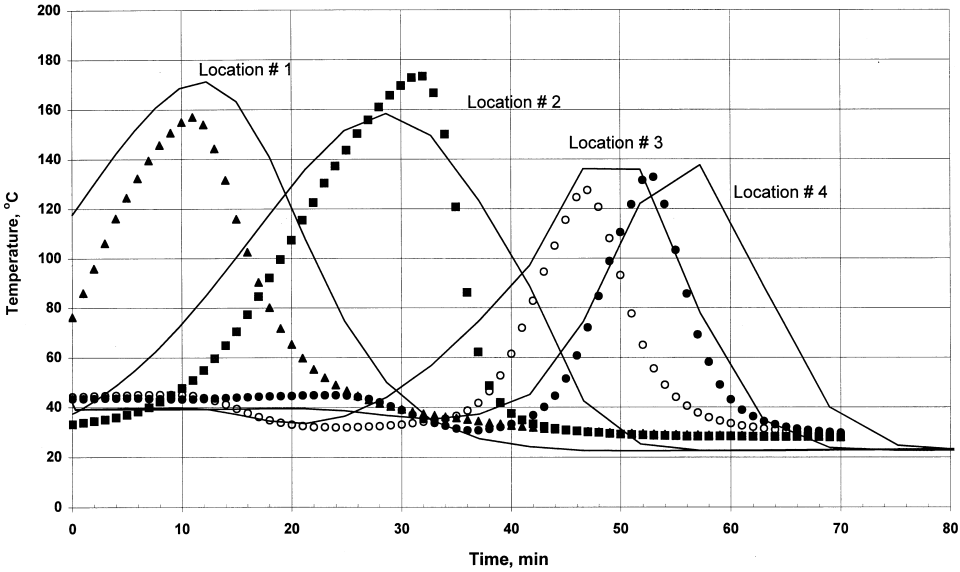


FIG. 2 Thermal pulses inside a PPU bed at different axial locations: Plant test data points = experimental, solid lines = simulator predictions.



## Case Study

The above simulator was then used to compare the following process options:

1. Increase the ratio of cooling to heating time ($t_c : t_h$),
2. Repressurization by the feed air from the feed end or by the PPU product from the product end of the vessel,
3. Add another step in the cycle: simultaneous production step (duration = $t$_Sim). During this step, the adsorbent beds, the bed that was just repressurized, and the bed that was already on-line, are fed. Addition of this step does *not* reduce the magnitude of the thermal pulse exiting from the bed that was just put on the feed step. However, it results in mixing the effluent from the two beds, one of which has been on-line for some time and therefore is producing air at close to the feed temperature. This results in the combined effluent from the TSA PPU system entering the downstream equipment at a temperature cooler than if only the newly regenerated, repressurized bed was put on-line. The process cycle concept is illustrated in Fig. 3.

For all cases it was ensured that the beds were of the same size and were fully regenerated before starting the next cycle. For all the simulated cases, the

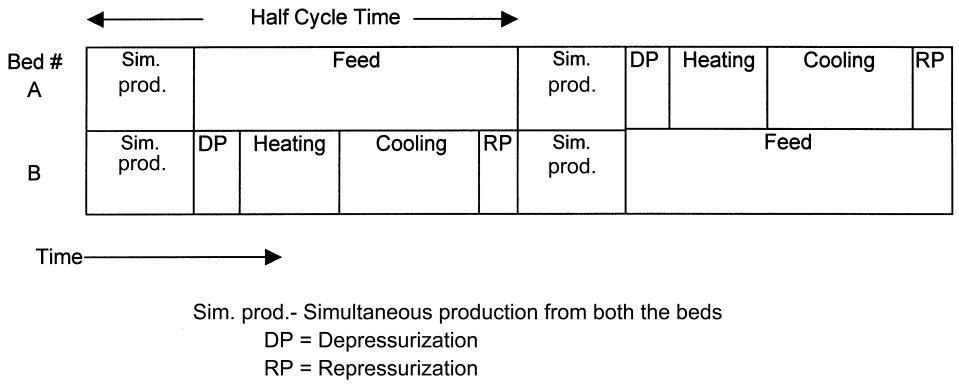


FIG. 3 Suggested cycle with simultaneous production step.



operating conditions, the adsorbent bed size, and the duration of the process steps are listed in Table 2.

### 1. Effect of Cooling-to-Heating-Time Ratio ($t_c$: $t_h$): Product End Repressurization

For all cases in this option, the simultaneous production step duration ($t$_Sim) was fixed at 5 min. This is usually the minimum time used in such processes to accommodate for the closing and opening of the valves. Eight cases were simulated from $t_c : t_h = 0.8$ to $t_c : t_h = 3.0$. This covers the range of this variable most commonly used in these types of units. Temperature profiles exiting the PPU bed during the feed step are shown in Fig. 4. The effluent temperature profiles are the result of mixing the gas from two beds: one that was already on-line and the other that was recently put on-line after the regeneration and the repressurization steps. During the initial time (~4 min) there was no effect of $t_c : t_h$ on the outlet temperature. After that, the temperature rose in

TABLE 2
Operating Conditions for the Simulated Options

| | | |
|---|---|---|
| Feed pressure | 20.7 | bara |
| Feed temperature | 7.2 | °C |
| Feed flow rate | 83,300 | SCMH |
| Regeneration temperature | 204 | °C |
| Total adsorbent weight | 10,520 | kg/bed |
| Vessel ID | 3.44 | m |
| Vessel T-T | 1.83 | m |
| Depressurization step duration | 20 | min |
| Repressurization step duration | 20 | min |
| Half cycle time | 365 | min |

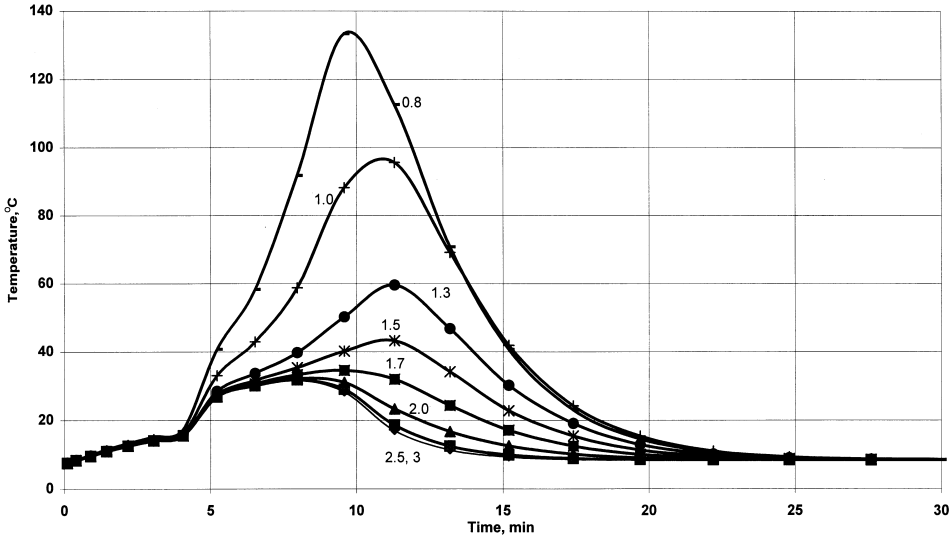


FIG. 4 Thermal pulse from PPU system—Product-end repressurization; effect of $t_c : t_h$: t_Sim = 5 min.



two pulses; the first thermal pulse was caused by the repressurization step, followed by the second, and more pronounced, thermal pulse caused by insufficient cooling of the bed. As $t_c : t_h$ increased the second peak, caused by the insufficient cooling of the bed, decreased. After $t_c : t_h \sim 1.7$, this peak was almost eliminated and the only remaining peak was the one caused by PPU product repressurization. Table 3 lists the regeneration gas-flow requirements for

TABLE 3
Dependence of Regeneration Flow Rate and PPU Effluent Peak Temperature on $t_c : t_h$
(Simultaneous Production Step Duration, t_Sim = 5 min)

| Ratio of cooling to heating time $t_c : t_h$ | Ratio of regeneration flow rate | Peak temperature, °C | |
|---|---|---|---|
| | | Product-end repressurization | Feed-end repressurization |
| 0.8 | 0.90 | 133.3 | 124.4 |
| 1 | 1.00 | 96.1 | 77.2 |
| 1.3 | 1.15 | 59.4 | 43.9 |
| 1.5 | 1.25 | 43.3 | 36.7 |
| 1.7 | 1.35 | 34.4 | 33.3 |
| 2 | 1.50 | 33.3 | 32.2 |
| 2.5 | 1.75 | 33.3 | 31.7 |
| 3 | 2.00 | 33.3 | 31.7 |

these eight cases. The regeneration gas requirement increased as $t_c : t_h$ increased. The minimum requirement was at $t_c : t_h = 0.8$. However, the peak PPU product temperature for this case was ~135°C. This is unacceptable for most ASU plants.

### 2. Effect of Cooling-to-Heating-Time Ratio ($t_c : t_h$): Feed End Repressurization

Similar to the previous option, the simultaneous production step duration ($t$_Sim) was fixed at 5 min for this option. Eight cases were simulated from $t_c : t_h = 0.8$ to $t_c : t_h = 3.0$. Temperature profiles exiting the PPU bed during the feed step are shown in Fig. 5. Very similar trends, as for the previous option (product-end repressurization), were observed. However, two exceptions are noted. First, for all cases the peak temperature was lower for feed-end repressurization than for product-end repressurization. Second, the duration of the thermal pulse was shorter for this option than for the product-end repressurization option. It should be pointed out that for most cases, the safety of the downstream equipment was most significantly affected by the peak temperature of the thermal pulse; however, the performance of the downstream equipment was effected by both the peak and the duration of the thermal pulse.

Figure 6 compares the PPU effluent temperature for the product-end and the feed-end repressurization cases at tc : th = 1.0 and t_Sim = 5 min. It is clear

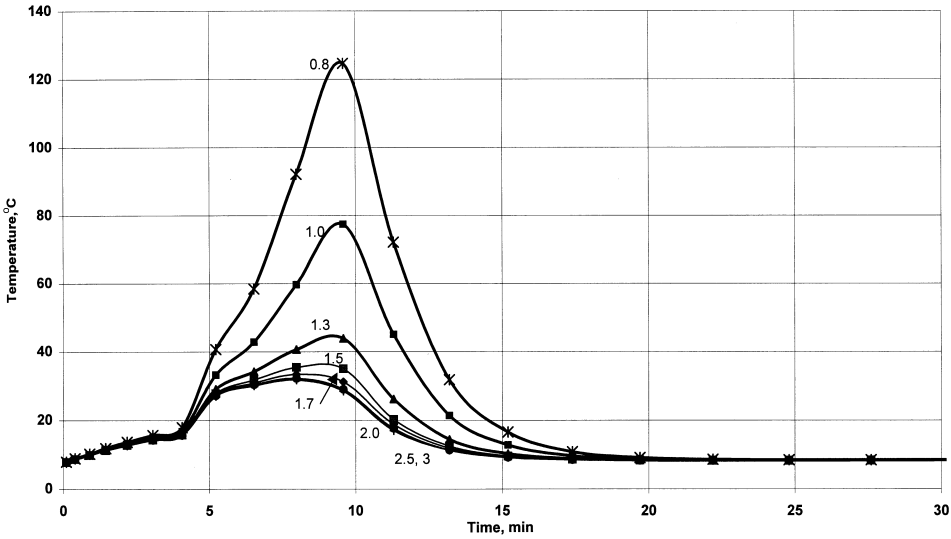


FIG. 5 Thermal pulse from PPU system—feed-end repressurization; effect of $t_c : t_h$: t_Sim = 5 min.

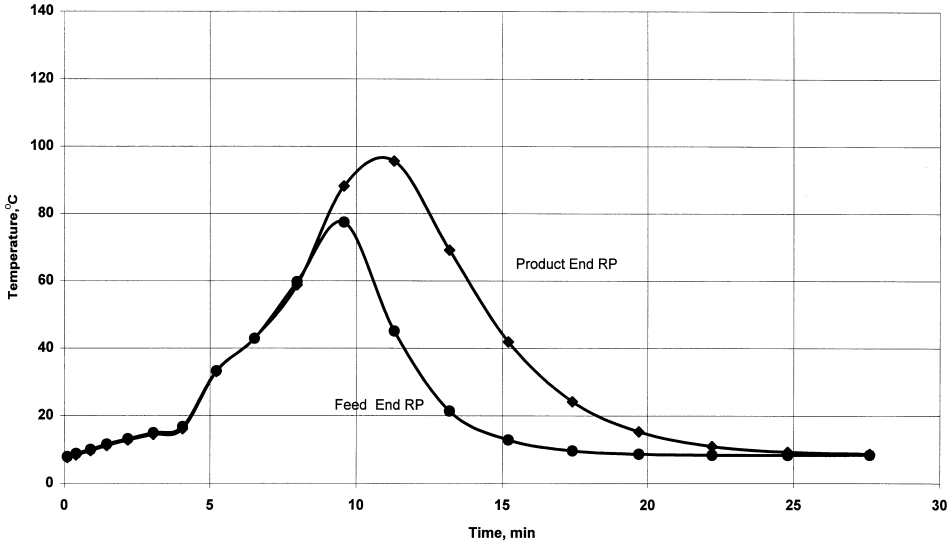


FIG. 6 Thermal pulse from PPU system—feed- vs. product-end repressurization; $t_c : t_h$: = 1.0, t_Sim = 5 min.



from Fig. 6 that the thermal pulse for the product repressurization case has a higher peak and is more spread out than for the feed-end repressurization option. To further explore the reasons for these differences, temperature profiles along the adsorbent bed are plotted at the end of the heating and cooling steps (Fig. 7), at the end of the repressurization steps (Fig. 8), and at the end of the 5 min simultaneous production steps (Fig. 9) for these two cases. Figure 7 shows that the temperature profiles at the end of the heating and cooling steps are identical. This is expected, because the amount of feed processed and regeneration conditions were identical. Figure 8 shows that at the end of the repressurization step, the product end of the bed was cooler by ~35°C for the product-end repressurization option than for the feed-end repressurization option. However, for the feed-end repressurization option, the feed end of the bed was cooler by ~135°C than it was for product-end repressurization. This is the direct result of the product temperature in TSA PPUs being higher than the feed temperature, due to the heat of adsorption for the trace impurities. However, this difference in bed temperature profiles at the end of the repressurization steps implies that for the feed-end repressurization option the bed is cooler at the end of the repressurization step than it is for the product-end repressurization option. This difference results in a higher and more-spread-out peak inside the bed for the product-end repressurization option at the end of the 5 min simultaneous production step as shown in Fig. 9. When this tem-

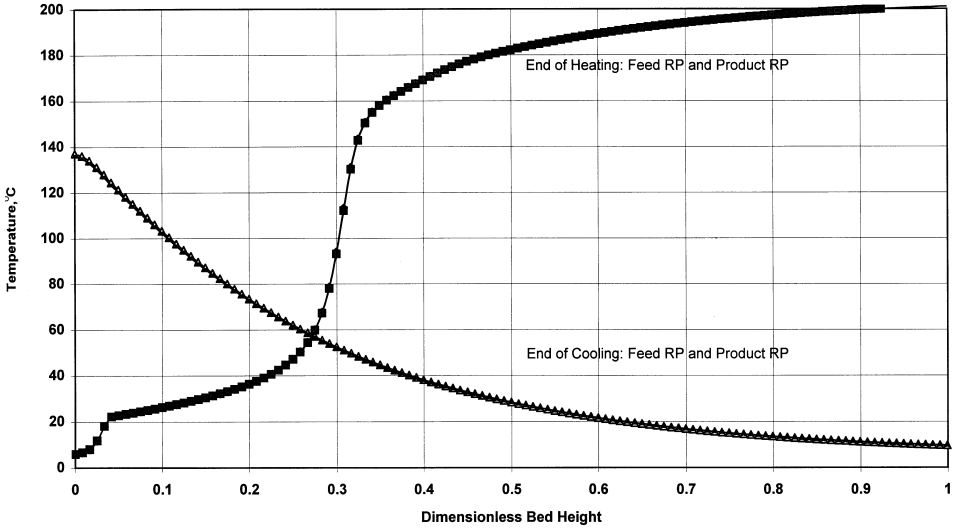


FIG. 7 Temperature profiles inside the bed; $t_c : t_h = 1.0$, t_Sim = 5 min.



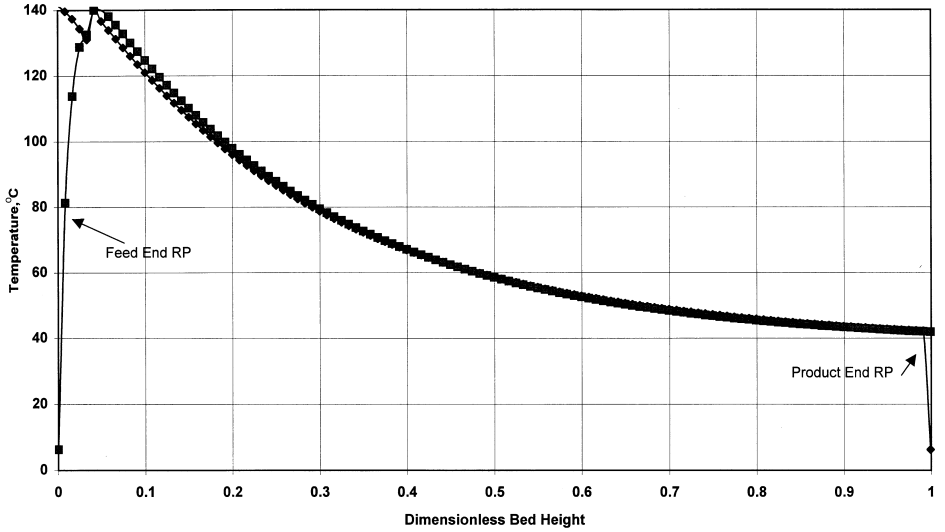


FIG. 8 Temperature profiles inside the bed: end of repressurization; $t_c : t_h = 1.0$, t_Sim = 5 min.

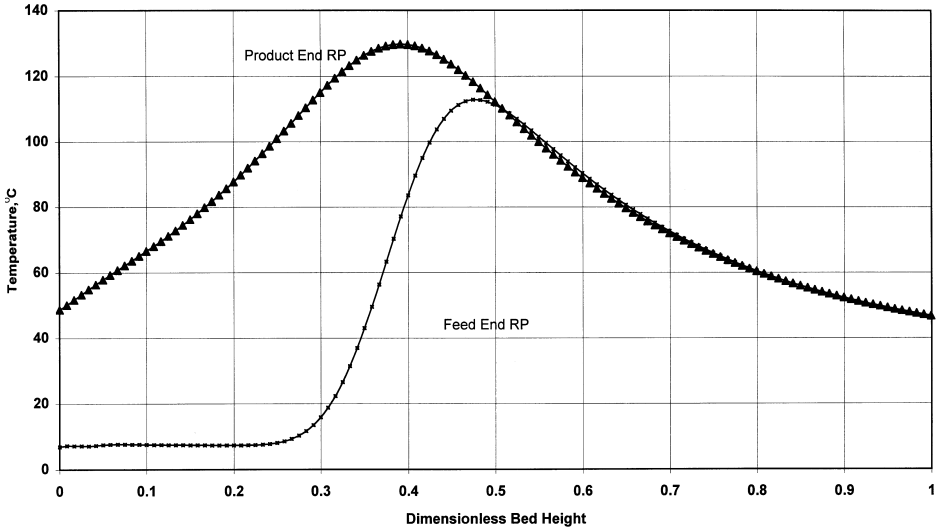


FIG. 9 Temperature profiles inside the bed: end of simultaneous production step; $t_c : t_h = 1.0$, t_Sim = 5 min.



perature profile exits the bed and is mixed with the cooler effluent from the other bed for 5 min, the overall effluent temperature as demonstrated in Fig. 6 results.

Because the adsorbents used in TSA PPUs have a strong affinity for trace impurities, the direction of repressurization (product or feed-end) has no impact on the process performance.

### *3. Effect of Increasing the Duration of the Simultaneous Production Step (t_Sim)*

The process cycle for this option is illustrated in Fig. 3. Eight cases were simulated with t_Sim = 5 to 110 min. For all the cases $t_c : t_h = 1.0$ was chosen, and the repressurization was from the feed end. During the simultaneous production step each bed was fed about half the normal feed flow rate. The thermal pulse coming out of the PPU system during the entire simultaneous production step was the result of temperature obtained by mixing the effluent product streams from both the beds, only one of which had residual heat. Results for the simulated cases are plotted in Fig. 10. The exit temperature profiles were quite different than for the previous two options. Two separate pulses were not observed after t_Sim ~10 min. As t_Sim increased the location of the peak shifted to the right and its magnitude dropped. There

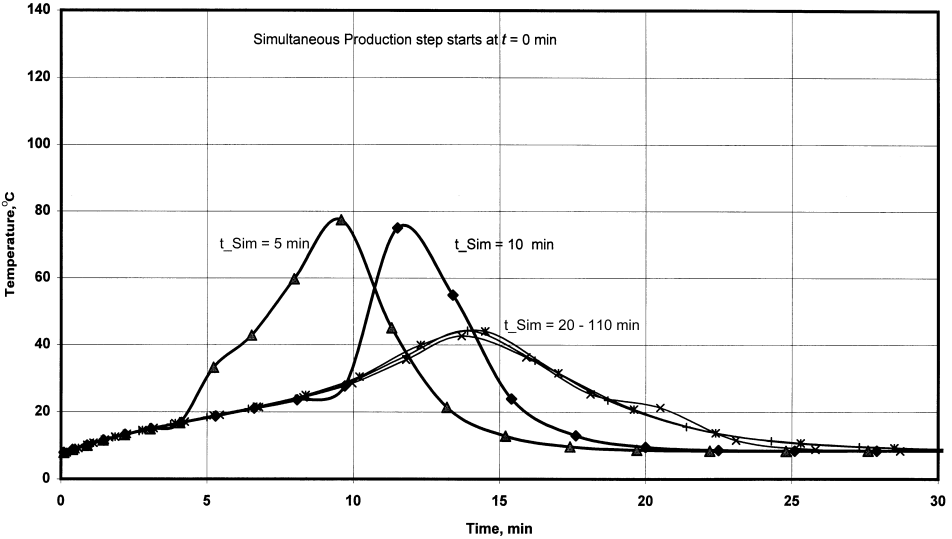


FIG. 10 Thermal pulse from PPU system—effect of simultaneous production step duration $t_c$ : $t_h = 1.0$, feed-end repressurization.



was no significant drop in peak temperature after t_Sim was increased above 20 min.

To further understand this behavior, temperature profiles inside the bed at different times in the cycle are plotted. Figure 11 compares the temperature profiles for various cases (t_Sim = 5, 10, 20, and 110 min) at the end of the feed-end repressurization steps. As expected, all the temperature profiles are almost identical. Figure 12 compares the temperature profiles inside the bed at the end of the simultaneous production step. The temperature profile for t_Sim = 10 min is farther down the bed than the temperature profile for t_Sim = 5 min. However, for both the cases, the temperature peaks are left inside the bed at the end of the simultaneous production steps. At the end of this step, the feed flow rate is increased to the full normal flow rate through the bed. The temperature peaks then starts to come out from the bed (Fig. 10) for these two cases. However, the product from the recently regenerated bed no longer has the advantage of mixing with the product from the bed, which has been on-line for some time and is producing cooler effluent in both cases. Therefore, the peak temperature in the exit stream from the system is not only significantly affected, it arrives at the exit at a later time for the t_Sim = 10 min case.

For t_Sim $\geq$ 20 min, the temperature peak has already exited the bed during the simultaneous production step (Fig. 12). Therefore, the effluent with

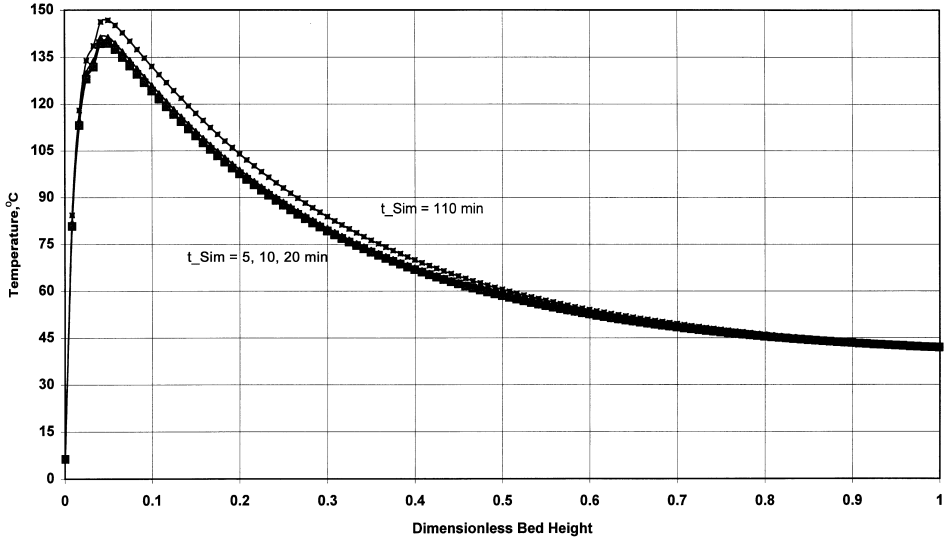


FIG. 11 Temperature profiles inside the bed at the end of repressurization Step—effect of simultaneous production step duration; $t_c : t_h = 1.0$, feed-end repressurization.

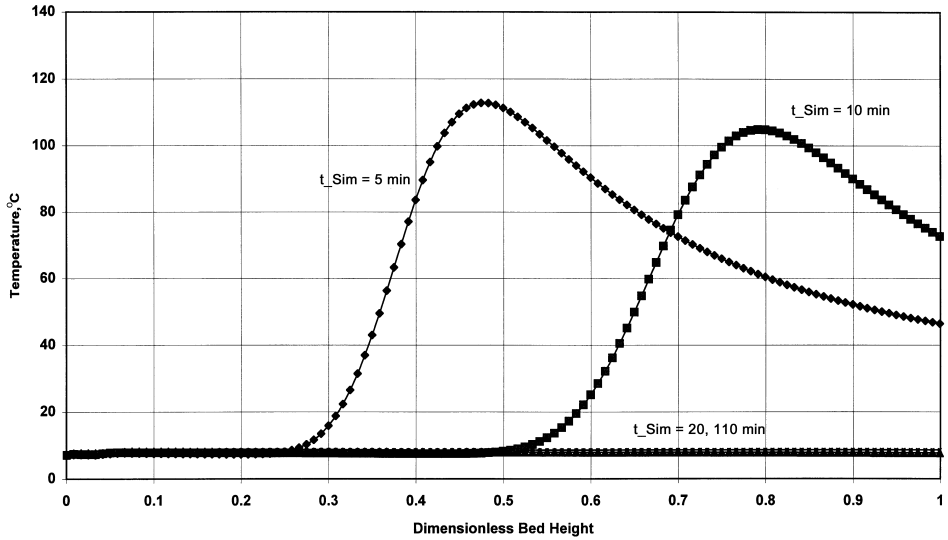


FIG. 12 Temperature profiles inside the bed at the end of simultaneous production step—effect of simultaneous production step duration; $t_c : t_h = 1.0$, feed-end repressurization.

peak temperature from this bed mixes with the product from the bed, which has been on-line for some time and has been producing the cooler effluent. No extra residual heat is left inside this bed at the end of the simultaneous production step. Therefore, no further temperature reduction in the effluent from the PPU system is possible by mixing the effluent from these two beds after t_Sim $\geq$ 20 minutes. This results in the mixed effluent temperature profile are the same for all cases after t_Sim $\geq$ 20 min, as shown in Fig. 10, at these operating conditions.

## CONCLUSIONS

The peak temperatures exiting the PPU system are plotted as a function of regeneration gas-flow rate for the three options: $t_c : t_h$ variations for the feed-end repressurization, $t_c : t_h$ variations for the product-end repressurization, and extended t_Sim options in Fig. 13. Coupled with Tables 3 and 4, it is observed that:

1. Peak temperatures are lower for the feed-end repressurization option.
2. At t_Sim = 5 min, $t_c : t_h \geq 1.5$ results in minimum peak temperature from the PPU system. However, the regeneration gas requirement is 25% more than the minimum.
3. There is no reduction in the minimum peak temperature by increasing t_Sim beyond 20 min at these operating conditions.



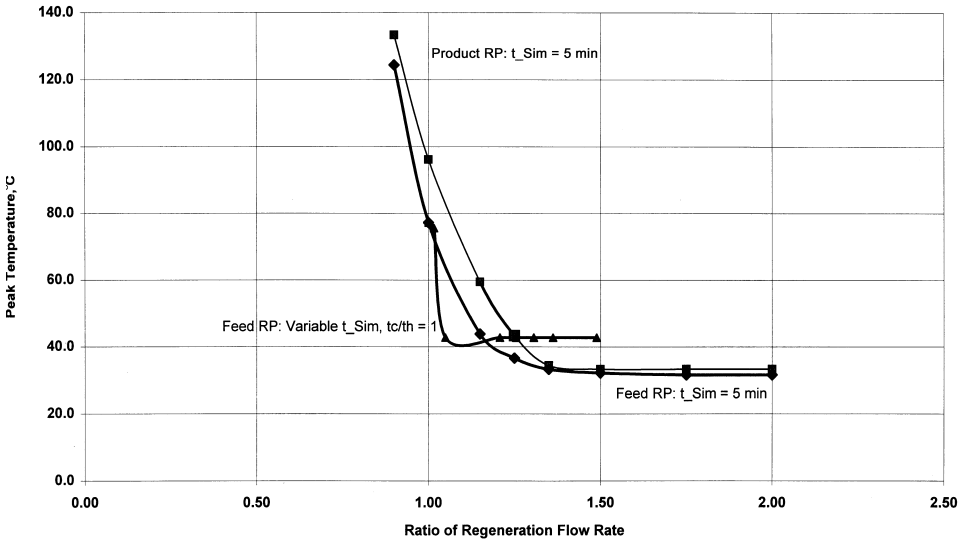


FIG. 13 Peak temperature as a function of regeneration gas flow rate.

TABLE 4
Dependence of Regeneration Flow Rate and PPU Effluent Peak Temperature on t_Sim
(Repressurization Direction: from the Feed-End Cooling-to-Heating-Time Ratio, $t_c : t_h = 1$)

| Simultaneous production step duration t_Sim, min | Ratio of regeneration flow rate | Peak temperature, °C | Ratio of power consumption |
|---|---|---|---|
| 5 | 1.00 | 77.2 | 1.00 |
| 10 | 1.02 | 75.6 | 1.01 |
| 20 | 1.05 | 42.8 | 1.04 |
| 60 | 1.21 | 42.8 | 1.18 |
| 70 | 1.25 | 42.8 | 1.22 |
| 80 | 1.31 | 42.8 | 1.26 |
| 90 | 1.36 | 42.8 | 1.31 |
| 110 | 1.49 | 42.8 | 1.41 |



4. The regeneration gas requirement is minimum at t_Sim = 20 min at these operating conditions. However, the power requirement is ~4% higher (Table 4). This may be the best option if peak temperature of ~43°C is acceptable for the downstream equipment.

The overall PPU system design will depend on the economic evaluation of all possible options. However, such an evaluation may not be possible without a simulator to differentiate between various options. Therefore, an advanced simulator is essential to compare various options, because some of these results cannot be arrived at by intuition. Also, the exact value of *t*_Sim will depend on the operating conditions of the TSA PPU.

## NOMENCLATURE

| | |
|---|---|
| $C$ | total molar concentration of the gas |
| $C_w$ | heat capacity of the wall |
| $C_i$ | $= \frac{P_i}{RT}$, molar concentration of component $i$ in the gas mixture |
| $C_{io}$ | initial molar concentration of component $i$ in the gas mixture |
| $c_p$ | heat capacity at constant pressure |
| $C_{pg}$ | heat capacity of the gas |
| $C_j^s$ | heat capacity of the adsorbent $j$ |
| $c_v$ | heat capacity at constant volume |
| $d_{\text{in}}$ | inside bed diameter |
| $d_{\text{out}}$ | outside bed diameter |
| $h_w$ | heat transfer coefficient between packed bed and the vessel wall |

| | |
|---|---|
| $K_j^i$ | rate of adsorption |
| $P$ | pressure |
| $P_{\text{from}}$ | pressure above the orifice in direction of the flow |
| $P_{\text{to}}$ | pressure down the orifice in direction of the flow |
| $P_{\text{cr}}$ | critical pressure |
| $Q_j^{i\text{eq}}$ | moles of component $i$ adsorbed by the adsorbent $j$ at equilibrium |
| $Q_j^i$ | moles of component $i$ adsorbed by the adsorbent $j$ |
| $R$ | gas constant |
| $S_j^i$ | adsorption rate of the component $i$ by adsorbent $j$ |
| $S_{\text{bed}}$ | bed cross-section |
| $S_{\text{orifice}}$ | orifice cross-section |
| $s(T)$ | sonic velocity at temperature $T$ |
| $t$ | time variable |
| $T$ | temperature |
| $t_c$ | duration of the cooling step |
| $T_{\text{from}}$ | temperature of the gas at the source of the flow |
| $t_h$ | duration of the heating step |
| $T_o$ | bed and wall initial temperature |
| $T_{\text{to}}$ | temperature of the downstream gas |
| $T_w$ | wall temperature |
| $u$ | interstitial velocity |
| $x$ | distance variable |
| $\Delta H_j^i$ | heat of component $i$ adsorption on adsorbent $j$ |
| $\rho_w$ | vessel wall metal density |
| $\varepsilon_j$ | external void fraction in the bed packed with adsorbent $j$ |
| $\rho_j$ | adsorbent $j$ bulk density |
| $\gamma$ | $= c_p : c_v$ |

### *Superscripts and Subscripts*

| | |
|---|---|
| $i$ | adsorbate or bed |
| $j$ | adsorbent |
| eq | at equilibrium |

## REFERENCES

1. D. Basmadijian, "On the Possibility of Omitting the Cooling Step in Thermal Swing Adsorption Cycles," *Canadian J. Chem. Eng., 53*, 234 (1975).
2. R. Kumar and G. R. Dissinger, "Non-Equilibrium, Non-Isothermal Desorption of Single Adsorbate by Purge," *Ind. Eng. Chem. Process Design Devel., 25*(2), 456 (1986).
3. R. Kumar, V. G. Fox, D. G. Hartzog, R. E. Larson, Y. C. Chen, P. A. Houghton, and T. Naheiri, "A Versatile Process Simulator for Adsorptive Separations," *Chem. Eng. Sci., 18*(49), 3115 (1994).

4. H. K. Rhee, R. Aris, and N. R. Amundsen, *First-Order Partial Differential Equations*, Vol. I, Prentice-Hall, Paramus, NJ, 1986.
5. K. Chen and W. E. Schiesser, *Manual No. 5 for DSS/2 Package*, Lehigh University, 1990.
6. A. C. Hindmarsh, "ODEPACK, A Systematized Collection of ODE Solvers," in *Scientific Computing* (R. S. Stepleman, et al., Eds.), North-Holland, Amsterdam, 1983, pp. 55–64.

*Received by editor August 30, 1999*
*Revision received March 2000*